

Polymerization of Two Unsymmetrical Isomeric Monomers Based on Thieno[3,4-*b*]thiophene Containing Cyanovinylene Spacers

Venkataramanan Seshadri and Gregory A. Sotzing*

Department of Chemistry and the Polymer Program, 97 North Eagleville Road,
Storrs, Connecticut 06269-3136

Received February 12, 2004. Revised Manuscript Received August 2, 2004

Two cyanovinylene-containing isomeric monomers were prepared by the Knoevenagel condensation of 4- and 6-formylthieno[3,4-*b*]thiophene with thiophene-2-acetonitrile, and these monomers were electrochemically polymerized to yield two low-band-gap (1.2 eV) conjugated polymers. The onsets for oxidation of the conjugated polymers were found to have shifted ca. 0.6 V higher compared to the parent poly(thieno[3,4-*b*]thiophene) and the onset for reduction increased by ca. 0.1 V. Both polymers, according to spectroscopic evidence, were found to be deep blue in the neutral state and transmissive sky blue in the oxidized form, and these polymers exhibit stable n-doping behavior.

Introduction

Lowering the band-gap of intrinsically conducting polymers (ICPs) has been one of the prime objectives in many research groups owing to potential applications of these materials in type III supercapacitors,¹ electrochromics,² photovoltaics,³ molecular electronics,⁴ etc. Several strategies have been adopted toward tuning the band-gap of these conjugated polymers such as raising or lowering the HOMO or LUMO levels via electron-rich substitutions or withdrawing groups,⁵ fused aromatic units to stabilize the quinonoid form,⁶ preparing polymers containing alternating donor and acceptor repeat unit structures,⁷ and introducing spacers between adjacent aromatic rings to reduce the steric hindrance between rings.⁸ Use of terminal electroactive aromatic units with ethylenic spacers possesses the advantage of monomers being polymerizable by elec-

trochemical methods along with some of the above-listed advantages.⁹ Cyano substitutions on one of the olefinic carbons of heteroaryleneethylene compounds have been known to further reduce the band-gap as a result of stabilization of the quinonoid form.¹⁰ Herein we report the synthesis and characterization of two isomeric monomers containing cyanovinylene spacer units between thieno[3,4-*b*]thiophene and thiophene. Poly(thieno[3,4-*b*]thiophene), a polymer containing fused thiophene repeat-units, was reported to have a very low band-gap of 0.85 eV.¹¹ While Ferraris¹² and Pomerantz¹³ have reported 2-substituted thieno[3,4-*b*]thiophenes, we first reported optically transparent electrochemically generated unsubstituted poly(thieno[3,4-*b*]thiophene).¹⁴ Thieno[3,4-*b*]thiophene has three α -positions which are well separated from each other and, thereby, it has been hypothesized that polymerization could lead to a branched/cross-linked conjugated polymer. In an attempt to further reduce the band-gap we have introduced cyanovinylene spacers by Knoevenagel condensation of two isomeric formyl thieno[3,4-*b*]thiophenes with 2-thiophene acetonitrile to prepare two isomeric monomers. We also report the electrochemical preparation of the polymers from these two monomers and their electrochemical characterization. The two isomeric forms of the monomers were found to show different absorption maxima, and cross-linking through the α -positions

* To whom correspondence should be addressed. E-mail: sotzing@mail.ims.uconn.edu.

(1) Rudge, A.; Davey, J.; Raistrick, J.; Gottesfield, S.; Ferraris, J. P. *J. Power Sources* **1994**, *47*, 89.

(2) Argun, A. A.; Cirpan, A.; Reynolds, J. R. *Adv. Mater.* **2003**, *15*, 1338.

(3) Marks, R. N.; Halls, J. J. M.; Bradley, D. D. C.; Friend, R. H.; Holmes, A. B. *J. Phys. Condens. Matter* **1994**, *6*, 1379.

(4) Donhauser, Z. J.; Mantooth, B. A.; Kelly, K. F.; Bumrm, L. A.; Monnell, J. D.; Stapleton, J. J.; Price, D. W., Jr.; Rawlerr, A. M.; Allara, D. L.; Tour, J. M.; Wiess, P. S. *Science* **2001**, *292*, 2303.

(5) (a) Jonas, F.; Schrader, L. *Synth. Met.* **1991**, *41–43*, 831. (b) Reynolds, J. R. *Macromolecules* **2000**, *33*, 7051. (c) Aqad, E.; Lakshminantham, M. V.; Cava, M. P. *Org. Lett.* **2001**, *3*, 4283. (d) Ferraris, J. P.; Lambert, T. L. *Chem. Commun.* **1991**, 1268.

(6) (a) Wudl, F.; Kobayashi, M.; Heeger, A. J. *J. Org. Chem.* **1984**, *49*, 3382. (b) Kobayashi, M.; Colaneri, N.; Boysel, M.; Wudl, F.; Heeger, A. J. *J. Chem. Phys.* **1985**, *82*, 5717.

(7) (a) Yamamoto, T.; Zhou, Z.; Kanbara, T.; Shimura, M.; Kizu, K.; Maruyama, T.; Nakamura, Y.; Fukuda, T.; Lee, B.-L.; Ooba, N.; Tomaru, S.; Kurihara, T.; Kaino, T.; Kubota, K.; Sasaki, S. *J. Am. Chem. Soc.* **1996**, *118*, 10389. (b) Brockmann, T. W.; Tour, J. M. *J. Am. Chem. Soc.* **1995**, *117*, 4437. (c) Zhang, Q. T.; Tour, J. M. *J. Am. Chem. Soc.* **1997**, *119*, 5065. (d) Zhang, Q. T.; Tour, J. M. *J. Am. Chem. Soc.* **1998**, *120*, 5356.

(8) (a) Jen, K.-Y.; Maxfield, M. R.; Shacklette, L. W.; Elsenbaumer, R. L. *Chem. Commun.* **1987**, 309. (b) Barker, J. *Synth. Met.* **1989**, *32*, 43.

(9) (a) Martinez, M.; Reynolds, J. R.; Basak, S.; Black, D. A.; Marynick, D. S.; Pomerantz, M. *J. Polym. Sci., Part B: Polym. Phys.* **1988**, *26*, 911. (b) Roncali, J.; Thobie-Gautier, C.; Elandaloussi, E.; Frere, P. *Chem. Commun.* **1994**, 2249. (c) Sotzing, G. A.; Reynolds, J. R. *Chem. Commun.* **1995**, 703.

(10) (a) Ho, H. A.; Brisset, H.; Frere, P.; Roncali, J. *J. Chem. Soc., Chem. Commun.* **1995**, 2309. (b) Sotzing, G. A.; Thomas, C. A.; Reynolds, J. R. *Macromolecules* **1998**, *31*, 3750.

(11) Hong, S. Y.; Marynick, D. S. *Macromolecules* **1992**, *25*, 4652.

(12) Neef, C. J.; Brotherston, I. D.; Ferraris, J. P. *Chem. Mater.* **1999**, *11*, 1957.

(13) Pomerantz, M.; Gu, X.; Zhang, S. X. *Macromolecules* **2001**, *34*, 1817.

(14) (a) Lee, K.; Sotzing, G. A. *Macromolecules* **2001**, *34*, 5746. (b) Sotzing, G. A.; Lee, K. *Macromolecules* **2002**, *35*, 7281–7286.

could possibly lead to multiple pathways for charge mobility and hence the polymer could be more stable.

Experimental Section

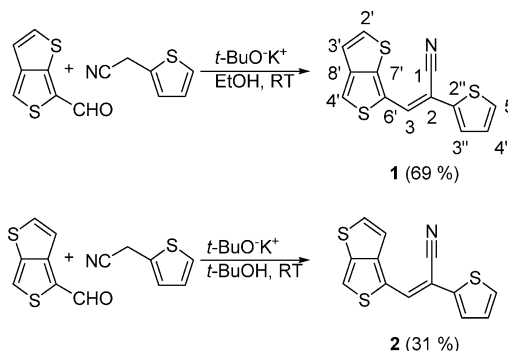
Chemicals. 4- and 6-Formyl thieno[3,4-*b*]thiophene were synthesized according to a previously reported procedure.¹⁵ Thiophene-2-acetonitrile was procured from Aldrich and distilled under reduced pressure before use. Potassium *tert*-butoxide was purchased from ACROS and used without further purification. Anhydrous ethanol was purchased from Fisher Scientific and used as received. Acetonitrile was purchased from Fisher scientific and freshly distilled over calcium hydride (ACROS) before use. Tetrabutylammonium perchlorate (TBAP) was prepared via addition of 70% perchloric acid solution (Fisher Scientific) to an aqueous solution containing a slight molar excess of tetrabutylammonium bromide. After filtration, the TBAP was recrystallized from ethanol, filtered, and dried under vacuum.

Caution. Perchloric acid is a powerful oxidant and hence requires great care for storage and use. In general, organic perchlorates should be handled with great care.

Instrumentation. ¹H and ¹³C NMR spectra were recorded on a Bruker 400 FT-NMR spectrometer. ¹H NMR data are reported as (chemical shift (multiplicity: *s* = singlet, *d* = doublet, *dd* = doublet of doublet); integration; coupling constant (*J*) in Hz, atom label). ¹H and ¹³C chemical shifts are reported in ppm downfield from tetramethylsilane (TMS) reference using the residual protonated solvent resonance as an internal standard. Infrared spectroscopy of the monomers was carried out using a Nicolet 560 spectrophotometer with KBr pellets. All optical studies were carried out using a Perkin-Elmer Lambda 900 UV-Vis-NIR spectrophotometer and the raw data obtained from the UV-Winlab software was plotted using Microcal Origin 6.0. Indium-doped tin oxide (ITO) coated glass with a nominal resistance of 15–25 ohms/sq (dimension 7 mm × 50 mm × 0.7 mm) was purchased from Delta Technologies, Ltd. and used for obtaining polymer absorbance spectra. All the electrochemical experiments were carried out on a CH Instruments 400 potentiostat, and the raw data were plotted using Microcal Origin 6.0. Gravimetric studies using the electrochemical quartz crystal microbalance (EQCM) were done using an oscillator circuit attached to a CH Instruments 400 potentiostat. The reference electrode used was a nonaqueous Ag/Ag⁺ electrode that was calibrated to be 0.45 V vs normal hydrogen electrode (NHE) using the ferrocene/ferrocenium couple.

Synthesis of Cyanovinylenes. (*E*)-3-(thieno[3,4-*b*]thiophen-6-yl)-2-(thiophen-2-yl)acrylonitrile (**1**). To a 100 mL vacuum-dried and argon purged round-bottom flask, thiophene-2-acetonitrile (0.123 g, 1 mmol) in 10 mL of anhydrous ethanol and potassium *tert*-butoxide (0.112 g, 1 mmol) in 10 mL of ethanol were added and stirred for 15 min at room temperature. To this solution, a 10-mL solution of 6-formylthieno[3,4-*b*]thiophene (0.168 g, 1 mmol) in ethanol was added, upon which the reaction mixture turned red. The reaction was continued at room temperature for 20 h under argon and was added to 30 mL of ice-water yielding **1** as a yellow solid. The solids were filtered, washed with 50 mL of water, and dried under vacuum (0.1 Torr) at room temperature for 24 h to give 0.188 g (69%) of pure **1**. Light yellow solid, mp 132–133 °C. GC-MS: Single peak with *m/z* 273 (M⁺). ¹H NMR (400 MHz, CDCl₃): δ 7.57 (s; 1H; H-4'), 7.52 (s; 1H; H-3), 7.40 (d; 1H; *J* = 5.51 Hz; H-2'), 7.34 (dd; 1H; *J* = 3.67 Hz, 1.0 Hz; H-3''), 7.30 (dd; 1H; *J* = 5.10 Hz, 1.1 Hz; H-5''), 7.07 (dd; 1H, *J* = 5.11 Hz, 3.67 Hz; H-4''), 6.97 (d; 1H; *J* = 5.52 Hz; H-3'). ¹³C NMR (400 MHz, CDCl₃): δ 145.5 (C-7'), 145.5 (C-3), 146.9 (C-8'), 139.0 (C-2''), 132.1 (C-2'), 128.5 (C-4''), 126.9 (C-3''), 126.1 (C-5''), 123.5 (C-6'), 117.5 (C-3'), 117.5 (C-2), 117.3 (C-4'), 101.8 (C-1). FTIR (KBr, cm⁻¹): 3092 (aromatic C-H stretching), 2214 (C≡N stretching), 1576 & 1446 (C=C stretching), 1336,

Scheme 1. Synthesis of **1** and **2**



Atom labels are shown for **1**.

1242 (in-plane C-H bending), 867, 849, 713, 662 (out-of-plane bending). UV in acetonitrile: 233 nm ($\epsilon = 19\,000\text{ Lmol}^{-1}\text{cm}^{-1}$), 275 nm ($\epsilon = 15\,000\text{ Lmol}^{-1}\text{cm}^{-1}$), 389 nm ($\epsilon = 17\,000\text{ Lmol}^{-1}\text{cm}^{-1}$).

(*E*)-3-(thieno[3,4-*b*]thiophen-4-yl)-2-(thiophen-2-yl)acrylonitrile (**2**). Compound **2** was prepared from 4-formylthieno[3,4-*b*]thiophene by a similar procedure but using *tert*-butyl alcohol instead of ethanol. Some dark solids were found in the reaction mixture, which were filtered off before quenching the reaction in an ice-water mixture resulting in an orange-red solid. The solid was filtered and washed with water and dried under vacuum at room temperature for 24 h to give 85 mg (31%) of **2**. Orange-red solid, mp 136–138 °C. GC-MS: Single peak with *m/z* 273 (M⁺). ¹H NMR (400 MHz, CDCl₃): δ 7.73 (s; 1H, H-3), 7.54 (d; 1H; *J* = 5.58 Hz; H-2'), 7.49 (s; 1H; H-6'), 7.33 (dd; 1H; *J* = 3.67 Hz, 1.1 Hz; H-3''), 7.28 (dd; 1H; *J* = 5.11 Hz, 1.1 Hz; H-5''), 7.15 (d; 1H; *J* = 5.60 Hz; H-3'), 7.07 (dd; 1H, *J* = 5.11 Hz, 3.67 Hz; H-4''), 139.8 (C-7'), 139.3 (C-2''), 135.6 (C-2'), 130.7 (C-3), 128.5 (C-4''), 126.8 (C-3''), 125.9 (C-5''), 124.4 (C-4'), 116.5 (C-6'), 116.2 (C-3'), 101.1 (C-1). FTIR (KBr, cm⁻¹): 3083 (aromatic C-H stretching), 2206 (C≡N stretching), 1570 & 1434 (C=C stretching), 1332, 1300, 1246, 1215 (in-plane C-H bending), 748, 698 (out-of-plane bending). UV (in acetonitrile): 256 nm ($\epsilon = 2 \times 10^8\text{ Lmol}^{-1}\text{cm}^{-1}$), 311 nm (shoulder), 397 nm ($\epsilon = 3 \times 10^8\text{ Lmol}^{-1}\text{cm}^{-1}$).

Electrochemical Polymerization and Polymer Characterization. Polymers from **1** and **2** were prepared electrochemically on platinum button electrodes by potential cycling generally between -0.5 and 1.0 V (vs Ag/Ag⁺) or through constant potential experiments at the aforementioned potentials. N doping of the polymers was done in the presence of lithium hydride to remove interference of water. The polymer spectrum in the doped and neutral forms was obtained electrochemically by sequential oxidation of the polymer on ITO in a cuvette using silver wire, calibrated to be 0.2 V vs NHE and an ITO as the counter electrode. The spectrum of N-doped polymers was obtained in the presence of anhydrous calcium sulfate and under nitrogen purge at -1.65 V (vs Ag/Ag⁺). All potential values have been reported vs Ag/Ag⁺.

Results and Discussion

Synthesis and Optical Properties of the Monomers. Cyanovinylene spacers were introduced between thieno[3,4-*b*]thiophene and thiophene by Knoevenagel condensation of the 4- and 6-formyl T34bT and 2-thiophene acetonitrile in accordance with Scheme 1.

The compounds **1** and **2** were obtained as pure compounds without any additional purification steps and were characterized using melting point, Fourier transform infrared (FTIR), electron impact gas chromatography/mass spectrometry (EI-GC/MS), and ¹H and ¹³C nuclear magnetic spectroscopy (NMR). NMR peak assignments were made using heteronuclear multiple

(15) Wynberg, H.; Feijen, J. *Recl. Trav. Chim. Pays-Bas* **1970**, *89*, 77.

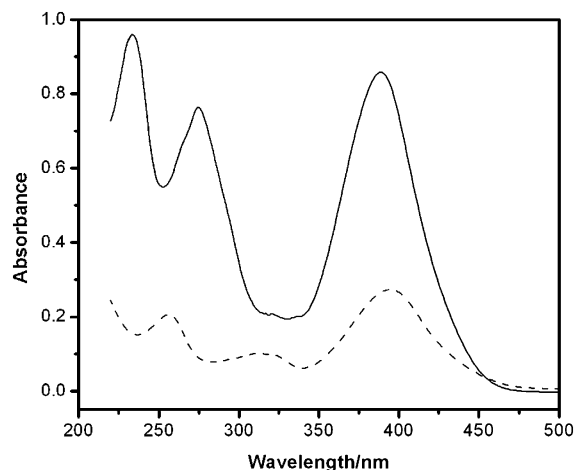


Figure 1. UV-vis absorption spectra of 50 μM of **1** (dashed line) and 5 nM of **2** (solid line) in acetonitrile.

bond correlation (HMBC), heteronuclear multiple-quantum coherence (HMQC), and nuclear Overhauser effect (NOE) NMR spectroscopy. 1D NOE experiments indicated that the heteroaromatic rings across the olefinic bonds are in the trans conformation in both the monomers as shown in Scheme 1. **2** was found to exhibit a lower energy absorption compared to **1** as observed from the UV-vis spectrum of the monomer solution in acetonitrile (Figure 1).

Figure 2 (A and B) shows the absorption and fluorescence emission spectra of **1** (excitation wavelength = 386) and **2** (excitation wavelength = 396 nm), respectively. The absorption maxima for the two monomers were in the blue region. The emission spectra show maxima in the bluish-green region at 445 and 480 nm for **1** and **2**, respectively.

Electropolymerization of 1 and 2. Poly(**1**) and poly(**2**) were electrochemically prepared using cyclic voltammetric polymerization between -0.4 and 0.9 V (vs Ag/Ag^+ reference electrode) at a scan rate of 100 mV/s from a 5 mM monomer solution in 0.1 M TBAP/acetonitrile. The cyclic voltammogram obtained for the electropolymerization of **2** is shown in Figure 3 and is representative for both the monomers.

The onset for the oxidation of **1** and **2** was ca. 0.7 V, while the peak potential for the two monomers was 0.83 and 0.79 V, respectively. The reduction of the polymer to the neutral form was found to occur between 0.7 and 0 V as seen in the reverse scan. During the second cycle an onset for oxidation occurs at a lower potential (ca. 0.1 V) due to the oxidation of the neutral conjugated polymer, and further scanning in the positive direction leads to a further increase in the anodic current above 0.7 V due to the oxidation of the monomer. The magnitude of the cathodic current is proportional to the amount of polymer being reduced and since this was found to be increasing with each cycle, it is indicative of additional polymer being deposited onto the working electrode during subsequent scanning and no passivation of the electrode was observed. The same results were confirmed using the electrochemical quartz crystal microbalance (EQCM). Figure 4 shows the cyclic voltammetric polymerization and concurrent gravimetry obtained for **1** during the first two cycles. A comparison of the cyclic voltammograms of the two monomers does

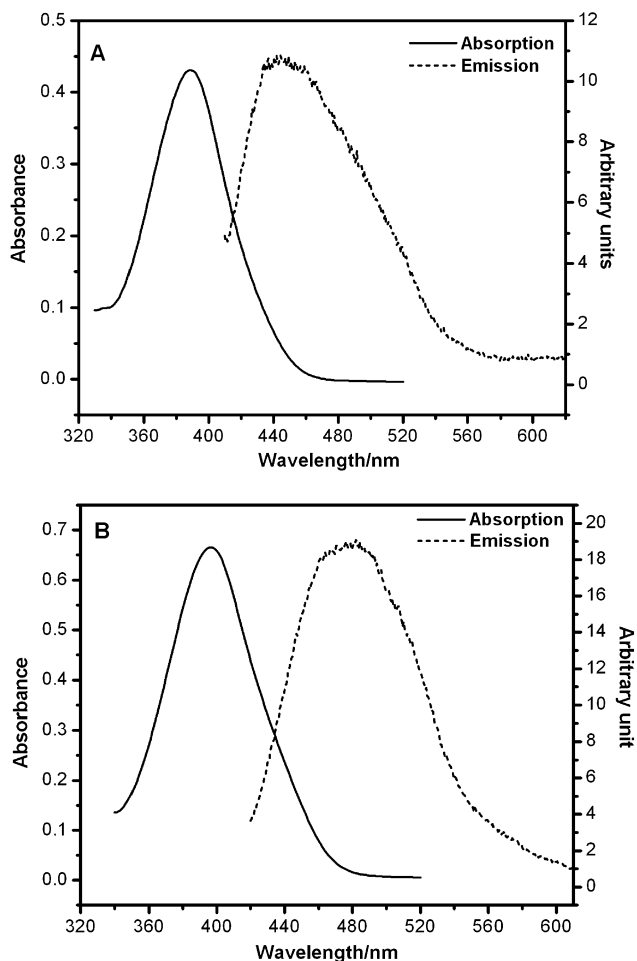


Figure 2. Absorption (solid line) and emission spectra (dotted line) of (A) **1** (excitation $\lambda = 386$ nm) and (B) **2** (excitation $\lambda = 396$ nm).

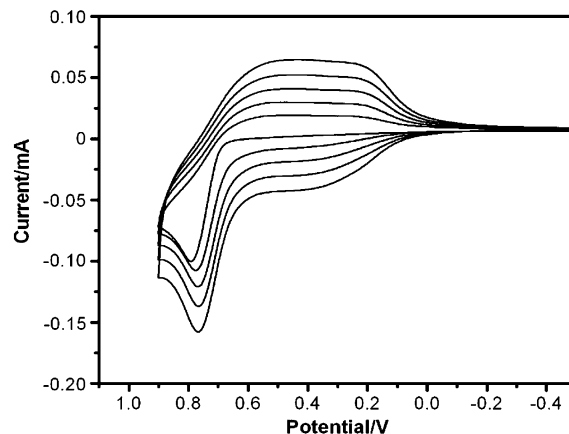


Figure 3. Cyclic voltammetry obtained during polymerization of 5 mM **2** in 0.1 M TBAP/ACN at a scan rate of 100 mV/s.

not show much change with respect to the monomers' oxidation potential or polymer reduction potential.

During the first anodic scanning an increase in mass was observed at ca. 0.7 V corresponding to the increase in the anodic current due to the oxidation of monomer and subsequent precipitation of the polymer onto the working electrode. Further positive scanning led to more polymer deposition as is observed in the gravimetric response. At 0.9 V, the scan was reversed but the polymer deposition continues until ca. 0.7 V as the

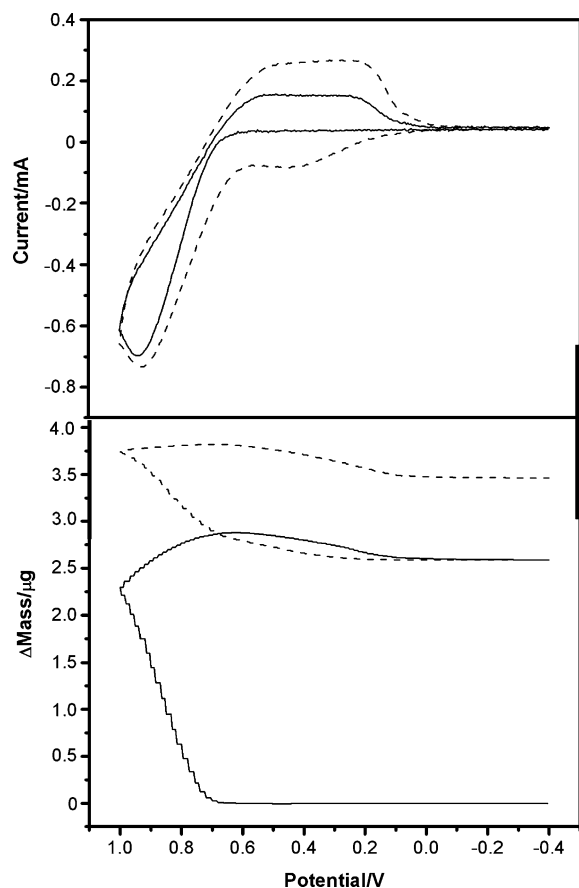


Figure 4. Cyclic voltammetry and concurrent gravimetry for the polymerization of **1** (5 mM) as observed using the EQCM in 0.1 M TBAP/ACN. First cycle (solid line), second cycle (dashed line).

potential is high enough for the oxidation of the monomer. Below 0.6 V a decrease in the mass is observed which can be attributed to predominant transport of the anions from the polymer film as the polymer is reduced to its neutral conjugated form. The mass decrease continues until 0 V and then reaches a steady state indicative of the complete reduction of the polymer. During the second scan an increase in the current and concurrent increase in the mass is observed at 0.1 V, which is attributed to the polymer oxidation. Further scanning in the positive direction leads to more monomer oxidation and subsequent polymer deposition, above 0.7 V, which is evident from the change in the slope of the gravimetric response. Although the current increases with increasing number of cycles (observed for as much as 5 cycles) in the cyclovoltammograms, the gravimetric response is reduced after the first cycle. Similar behavior was seen for **2** as well. Similar amounts of polymer had precipitated until ca. 0.9 V for the two monomers indicating similar polymer deposition rates. Again, during the second cycle of polymerization of **2** an increase in mass is evident at 0.1 V due to the oxidation of the precipitated polymer.

Polymer Electrochemistry. Poly(**1**) and poly(**2**) thus-produced by cyclic voltammetric polymerization were washed with acetonitrile and subjected to potential scanning in 0.1 M TBAP in ACN. Poly(**1**) shows reversible p-doping behavior between -0.2 and 0.9 V, while poly(**2**) shows reversible p-doping between -0.2 and 0.8 V. Furthermore, two discernible peaks are seen at 0.5

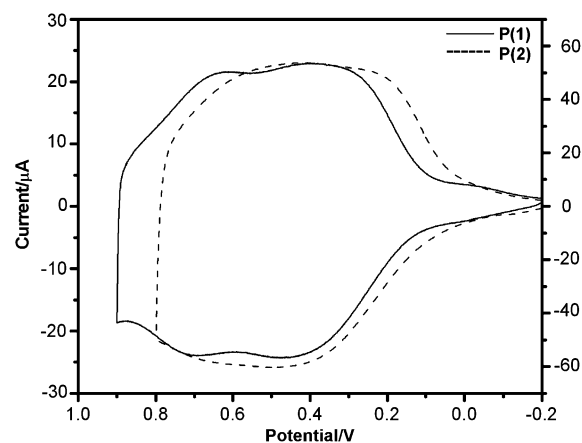


Figure 5. Cyclic voltammetry of poly(**1**) (solid line) and poly(**2**) (dashed line) on Pt at 100 mV/sec in 0.1 M TBAP/ACN.

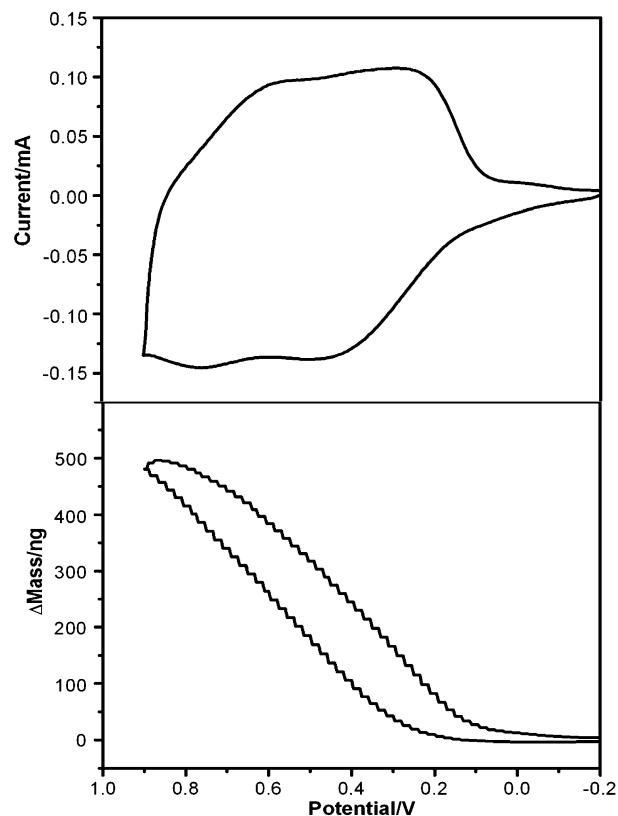


Figure 6. Cyclic voltammetry and concurrent gravimetry of poly(**1**) obtained using EQCM at a scan rate of 100 mV/sec in 0.1 M TBAP/ACN.

and 0.7 V for poly(**1**) while only one broad peak between 0.1 and 0.8 V is observed for poly(**2**) as shown in Figure 5. The onset for oxidation was found to occur at 0.15 and 0.1 V for poly(**1**) and poly(**2**), respectively. Both the polymers were cycled between -0.2 and 0.9 V at various scan rates and the current response was found to proportionally increase. The two polymers were found to be stable to redox stepping between constant potentials of -0.2 and 0.9 V retaining 80 and 85% electroactivity, respectively, after 500 redox-switching steps.

The polymer electrochemistry was studied via EQCM. As shown in Figure 6, a mass increase accompanies p-doping of poly(**1**) and upon de-doping, by a reversal of the scan, the mass drops owing to flux of ions out of the polymer film, a behavior typical for both polymers.

The ion transport is dominated by anions as evident by an increase in the mass during p-doping since the molar mass of the tetrabutylammonium cation is ca. 1.5 times greater than that of the perchlorate anion. A continuous increase in mass is observed until 0.9 V as the polymer is p-doped and upon reversing the scan the mass remains steady at the highest level of about 500 ng until 0.85 V and then starts decreasing as the anions move out of the film. This doping and de-doping process was reversible as seen in the cyclic voltammetry and gravimetry (Figure 6). Poly(1) and poly(2) were grown on gold coated quartz resonators by constant potential polymerization. The percent anion transport during p doping of the polymer was calculated to be 95% for both polymers from the chronocoulometric and concurrent chronogravimetric data obtained from the redox switching of both polymers using an earlier reported calculation method.¹⁶ The doping level calculated as the number of moles of electrons removed upon p doping per repeat unit of poly(1) and poly(2) were ca. 59% and 66%, respectively.

Freshly prepared poly(1) and poly(2) were washed with acetonitrile and dried under nitrogen. The polymers were then scanned between -1.6 and 0.9 V and between -1.5 and 0.8 V, respectively. The polymers were first anodically scanned until 0.9 and 0.8 V for poly(1) and poly(2), respectively (p doping), followed by a scan reversal. The cathodic scanning was further continued until -1.6 and -1.5 V for poly(1) and poly(2), respectively, to inject negative charges. Upon the first anodic scanning the onset for oxidation of poly(2) occurs at 0.1 V and the oxidation process continues as explained in the p doping process. At 0.8 V the scan is reversed and the polymer is reduced to the neutral form until ca. -0.2 V. Upon further cathodic scanning an increase in current is observed at -1.1 V with a peak at -1.5 V due to electron injection into the polymer. At -1.5 V the scanning is once again reversed in the anodic direction and the polymer is oxidized from the negatively charged form to the neutral form with a peak current for this process occurring at -1.25 V. On further anodic scanning two pre-peaks at -0.1 and 0.3 V are observed which have been attributed to the oxidation of trapped negative charges.¹⁷ Otero¹⁸ has reported that conjugated polymers, when oxidized for long periods of time and reduced at different potentials, give rise to a relaxation peak as a result of reopening the compacted structures. Thus, the prepeaks of Figure 7 could be a result of morphology change. During the subsequent cathodic scan of poly(2) a pre-peak possibly due to reduction of trapped positive charges is observed at -1 V and the peak current for the electron injection is observed at -1.44 V. The peak current for the electron injection process was found to decrease with increasing number of cycles with a retention of electroactivity (between -0.8 and 1.5 V), measured as the ratio of charge injected, of ca. 95% after five complete cycles. The band-gap for poly(2) was calculated from the difference between the onset of hole injection and

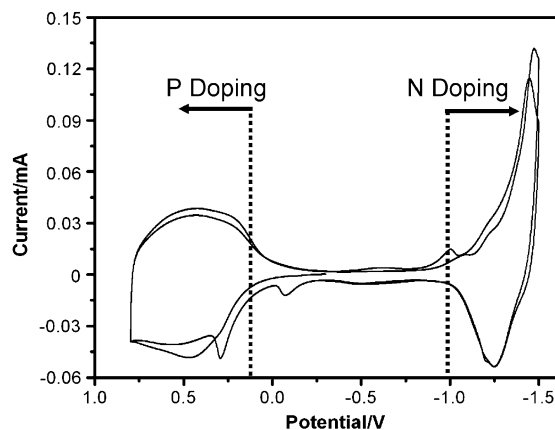


Figure 7. First two cyclic voltammograms obtained for the p and n doping of poly(2) in 0.1 M TBAP/ACN in the presence of lithium hydride.

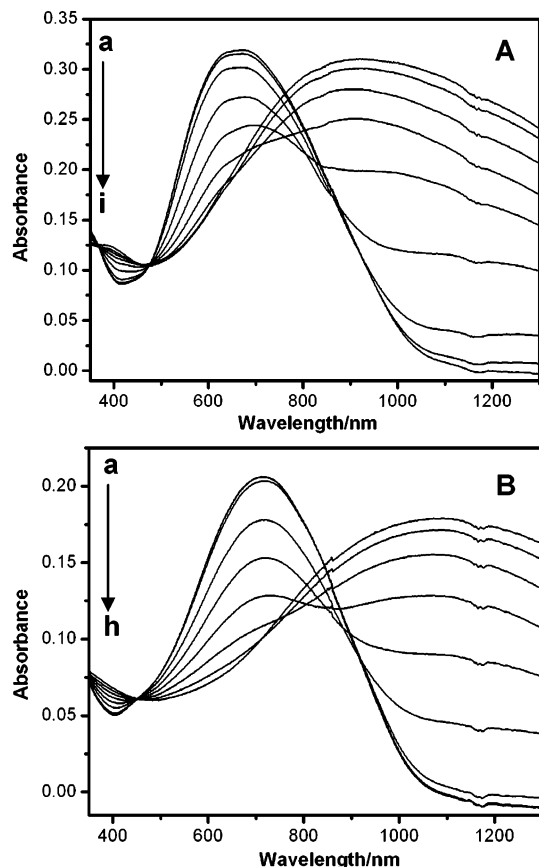


Figure 8. In situ spectroelectrochemistry of (A) Poly(1) at (a) -0.15 V, (b) 0.25 V, (c) 0.35 V, (d) 0.45 V, (e) 0.55 V, (f) 0.65 V, (g) 0.75 V, (h) 0.85 V, (i) 0.95 V; and (B) Poly(2) at (a) -0.45 V, (b) -0.05 V, (c) 0.25 V, (d) 0.45 V, (e) 0.55 V, (f) 0.65 V, (g) 0.75 V, and (h) 0.85 V in 0.1 M TBAP/ACN. Potentials are referenced against Ag/Ag^+ .

electron injection to be ca. 1.0 eV. Poly(1) showed similar hole and electron injection behavior with the exception that it had lower stability. Poly(1) only retained 73% electroactivity of the electron injection after five cycles. The band-gap for poly(1) was calculated from the onset of the hole and electron injection to be ca. 1.2 eV. Reynolds and co-workers¹⁹ have shown that some conjugated polymers exhibit electroactivity but not

(16) (a) Berlin, A.; Schiavon, G.; Zecchin, S.; Zotti, G. *Synth. Met.* **2001**, *119*, 153. (b) Seshadri, V.; Wu, L.; Sotzing, G. A. *Langmuir* **2003**, *19*, 9479.

(17) (a) Borjas, R.; Buttry, D. A. *Chem. Mater.* **1991**, *3*, 872. (b) King, G.; Higgins, S. J. *J. Mater. Chem.* **1995**, *5*, 447.

(18) Otero, T. F.; Padilla, J. J. *Electroanal. Chem.* **2004**, *561*, 167.

(19) DuBois, C. J.; Reynolds, J. R. *Adv. Mater.* **2002**, *14*, 1844.

semiconductive properties upon reduction. In situ spectroelectrochemical measurements in the vis-NIR region during n-doping were performed to examine if poly(**1**) and poly(**2**) exhibited behavior typical of a semiconductor.

In Situ Spectroelectrochemistry. Figure 8A and B show the spectra of poly(**1**) and poly(**2**) as a consequence of sequential electrochemical oxidation. With increasing positive potential, the absorption due to π to π^* transitions of the neutral polymer is found to decrease and a broad absorption extending into the NIR increases in intensity. The band-gaps of poly(**1**) and poly(**2**) are, as determined from the onset of the π to π^* transition of the neutral polymers, 1.20 eV (1035 nm) and 1.19 eV (1045 nm), respectively, with absorption maxima at 1.72 eV (720 nm) and 1.85 eV (669 nm). Both polymers are deep blue in the neutral conjugated form and transmissive sky blue in the oxidized form.

The vis-NIR spectra of poly(**1**) and poly(**2**) were obtained in the presence of anhydrous calcium sulfate under constant nitrogen purge. The vis-NIR spectrum of poly(**1**) and poly(**2**) were obtained at a constant potential of -1.65 V. The vis-NIR spectrum of poly(**1**) is shown in Figure 9 and was found to resemble the spectrum of the polymer in the p-doped state. Similar results were obtained for poly(**2**) as well. The absorbance extending through the NIR is characteristic of a semiconductor. Furthermore, the reversibility of these spectra was tracked using both potential stepping and cycling techniques. The insert in Figure 9 shows the reversibility of the change in absorbance measured at 669 nm during both p and n doping.

Conclusions

Two new cyanovinylene-containing monomers were prepared by the Knoevenagel condensation of 6- and 4-formylthieno[3,4-b]thiophenes with 2-thiopheneacetonitrile. These monomers have been electrochemically polymerized to produce two novel low-band-gap conjugated polymers. The band-gaps of the two polymers were deduced from the vis-NIR spectroscopy of the electrochemically obtained neutral polymers. Poly(**2**)

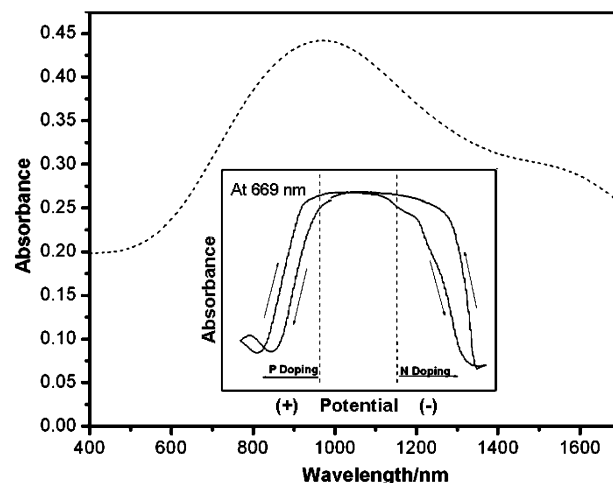


Figure 9. Vis-NIR spectrum of poly(**1**) in the n-doped form (-1.65 V, dashed line). Insert shows the change in absorbance at 669 nm (λ_{max} for the neutral poly(**1**)) as a function of scanning the potential from 0.8 V to -1.5 V).

was found to exhibit slightly lower energy absorption maxima (ca. 1.72 eV) compared to poly(**1**) (ca. 1.85 eV). The band-edge gap of the two polymers was approximately the same for both polymers at ca. 1.2 eV. The polymers were found to be highly stable to p-doping and moderately stable to n-doping in that there was only a 73% and 95% loss in electroactivity in going from the 1st to 5th cycle for poly(**1**) and poly(**2**), respectively. The band-gaps as calculated from the onsets for both p and n doping electrochemical processes were found to be 1.2 and 1.0 eV for poly(**1**) and poly(**2**), respectively. The polymers were found to be deep blue in the oxidized form and transmissive sky blue in the neutral state. Furthermore, the polymer was shown to exhibit similar vis-NIR absorption spectra in the p and n doped forms.

Acknowledgment. We acknowledge the American Chemical Society Petroleum Research Fund (Type G) for funding of this work.

CM049780R